Selective Gold Growth on CdSe Seeded CdS Nanorods

Gabi Menagen, David Mocatta, Asaf Salant, Inna Popov, Dirk Dorfs,* and Uri Banin

The Hebrew University of Jerusalem, Institute of Chemistry and the Center for Nanoscience and Nanotechnology, Givat Ram, Jerusalem 91904, Israel

Received June 22, 2008
Revised Manuscript Received September 29, 2008

Hybrid metal−semiconductor nanoparticles have attracted much attention recently. Metal tips on semiconductor nanorods can serve as anchor points for electrical connections and for self-assembly of complex structures.[1,2] Moreover, charge separation at the metal−semiconductor interface can be applied in photocatalytic processes.[3−5] Semiconductor/metal hybrid nanostructures have been synthesized from diverse combinations such as PbSe/Au,Ag or Pd,[6] CdSe/Au, CdS/Au,[7] TiO_2/Au,[3] CdSe/Co,[8] InAs/Au,[9] and TiO_2/Co.[10] For Au growth on CdSe nanorods, both two-sided and one-sided growth is possible. An electrochemical Ostwald ripening mechanism[11] was invoked to explain the transition from two to one-sided growth in these systems, where at a critical gold dot size, the small and less stable tip is oxidized and dissolved while the larger gold tip grows.[12] Here, we study the growth of Au on semiconductor rod heterostructures, more specifically on CdSe seeded CdS rods.[13−15] These high-quality nanorod heterostructures exhibit excellent optical properties that can be adjusted more controllably compared with one component systems.[16−18] Surprisingly, Au growth is selective to the position of the CdSe seed, and not to the CdS rod apexes or to defect sites as observed for simple CdS nanorods.[7] This behavior is assigned to an electrochemical Ostwald ripening process noted above, where the seed is a sink for electrons, thereby promoting Au growth in that region. This provides further evidence for the localization of the electrons in the seed region, consistent with recent scanning tunneling spectroscopy studies on these structures,[19] and unlike previous conjectures from elegant optical experiments. Additionally, the selectively located large gold dot on the rod may serve several purposes such as a seed for growth of other semiconductor structures[20] and an anchor point for self-assembly[2] and is of potential relevance for photocatalysis.[5]

The seeded growth approach of Manna et al. to synthesize CdSe seeded CdS rods was used.[15] Briefly, a precursor solution with CdSe dots as seeds and the sulfur precursor is rapidly injected into a solution of the cadmium precursor dissolved in a mixture of TOPO (*n*-trioctylphosphinoxide), TOP (*n*-trioctylphosphine) and phosphonic acids at 350−365 °C. After separation from the growth solution, subsequent gold growth is performed via a low-temperature reduction of $AuCl_3$ dissolved in toluene together with the seeded nanorods, DDA (dodecylamine) and DDAB (dodecyldimethylammonium bromide). Further details on the synthetic conditions are given in the Supporting Information.

Figure 1 shows transmission electron microscopy (TEM), high-resolution TEM (HRTEM), and high-angle annular dark field−scanning TEM (HAADF-STEM) images of the seeded nanorods before and after gold growth. The image of the CdSe seeded rods without gold (Figure 1a) shows that they are uniform in size (44 ± 8 nm long, 4.9 ± 0.7 nm wide). Figure 1c shows the same CdSe seeded nanorods with gold dots grown onto them identified clearly by the dark contrast. On most of the rods (78%), one large gold dot can be distinguished. The HAADF-STEM image of the same sample (Figure 1d) shows a much higher bright contrast for the gold than for the rest of the rod because of the z-contrast provided by this imaging method; the dominance of rods with a large gold dot is also obvious here. In few cases a significantly larger spot is not observed, whereas two larger spots on one rod were never observed. Remarkably, we find that the position of the larger gold spot is not distributed randomly on the rod. More precisely, the larger spot can neither be found on the end of the rod nor at the center of the rod.

* Corresponding author. E-mail: dirk@chem.ch.huji.ac.il.

(1) Mokari, T.; Rothenberg, E.; Popov, I.; Costi, R.; Banin, U. *Science* **2004**, *304* (5678), 1787–1790.
(2) Salant, A.; Amitay-Sadovsky, E.; Banin, U. *J. Am. Chem. Soc.* **2006**, *128* (31), 10006–10007.
(3) Subramanian, V.; Wolf, E. E.; Kamat, P. V. *J. Am. Chem. Soc.* **2004**, *126* (15), 4943.
(4) Ung, T.; Liz-Marzan, L. M.; Mulvaney, P. *J. Phys. Chem. B* **1999**, *103* (32), 6770–6773.
(5) Costi, R.; Saunders, A. E.; Elmalem, E.; Salant, A.; Banin, U. *Nano Lett.* **2008**, *8* (2), 637–641.
(6) Yong, K. T.; Sahoo, Y.; Choudhury, K. R.; Swihart, M. T.; Minter, J. R.; Prasad, P. N. *Nano Lett.* **2006**, *6* (4), 709–714.
(7) Saunders, A. E.; Popov, I.; Banin, U. *J. Phys. Chem. B* **2006**, *110* (50), 25421–25429.
(8) Kim, H.; Achermann, M.; Balet, L. P.; Hollingsworth, J. A.; Klimov, V. I. *J. Am. Chem. Soc.* **2005**, *127* (2), 544–546.
(9) Mokari, T.; Aharoni, A.; Popov, I.; Banin, U. *Angew. Chem., Int. Ed.* **2006**, *45* (47), 8001.
(10) Casavola, M.; Grillo, V.; Carlino, E.; Giannini, C.; Gozzo, F.; Pinel, E. F.; Garcia, M. A.; Manna, L.; Cingolani, R.; Cozzolli, P. D. *Nano Lett.* **2007**, *7* (5), 1386.
(11) Redmond, P. L.; Hallock, A. J.; Brus, L. E. *Nano Lett.* **2005**, *5* (1), 131–135.
(12) Mokari, T.; Sztrum, C. G.; Salant, A.; Rabani, E.; Banin, U. *Nat. Mater.* **2005**, *4* (11), 855–863.
(13) Talapin, D. V.; Koeppe, R.; Gotzinger, S.; Kornowski, A.; Lupton, J. M.; Rogach, A. L.; Benson, O.; Feldmann, J.; Weller, H. *Nano Lett.* **2003**, *3* (12), 1677–1681.
(14) Talapin, D. V.; Nelson, J. H.; Shevchenko, E. V.; Aloni, S.; Sadtler, B.; Alivisatos, A. P. *Nano Lett.* **2007**, *7* (10), 2951–2959.
(15) Carbone, L.; Nobile, C.; De Giorg, M.; Sala, F. D.; Morello, G.; Pompa, P.; Hytch, M.; Snoeck, E.; Fiore, A.; Franchini, I. R.; Nadasan, M.; Silvestre, A. F.; Chiodo, L.; Kudera, S.; Cingolani, R.; Krahne, R.; Manna, L. *Nano Lett.* **2007**, *7* (10), 2942–2950.
(16) Muller, J.; Lupton, J. M.; Lagoudakis, P. G.; Schindler, F.; Koeppe, R.; Rogach, A. L.; Feldmann, J.; Talapin, D. V.; Weller, H. *Nano Lett.* **2005**, *5* (10), 2044–2049.
(17) Shieh, F.; Saunders, A. E.; Korgel, B. A. *J. Phys. Chem. B* **2005**, *109* (18), 8538–8542.
(18) Kumar, S.; Jones, M.; Lo, S. S.; Scholes, G. D. *Small* **2007**, *3* (9), 1633–1639.
(19) Steiner, D.; Dorfs, D.; Banin, U.; Della Sala, F.; Manna, L.; Millo, O. *Nano Lett.* **2008**, *8* (9), 2954–2958.
(20) Sun, J. W.; Buhro, W. E. *Angew. Chem., Int. Ed.* **2008**, *47* (17), 3215–3218.

10.1021/cm801702x CCC: $40.75
Published on Web 10/24/2008

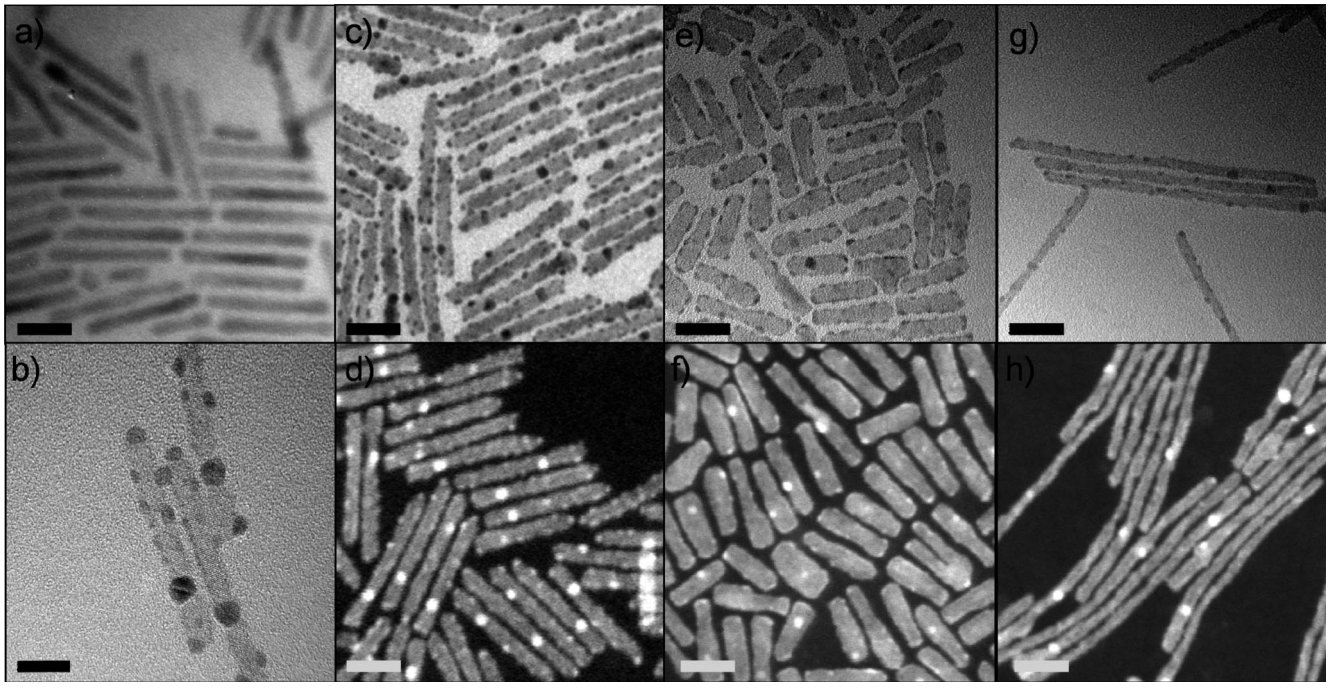

Figure 1. (a) CdSe seeded CdS nanorods (44 × 4.9 nm); (b) HR-TEM image of the rods with gold grown onto them; (c) image of medium-sized rods (44 × 4.9 nm) with gold growth; (d) HAADF-STEM image of the sample shown in c; (e) image of short thick rods (28 × 8 nm) with gold grown onto them; (f) HAADF-STEM image of the sample shown in e; (g) image of long thin rods (108 × 4.6 nm) with gold grown onto them; (h) HAADF-STEM image of the sample shown in g; the sizebar is 20 nm in all cases except b, where the bar is 10 nm.

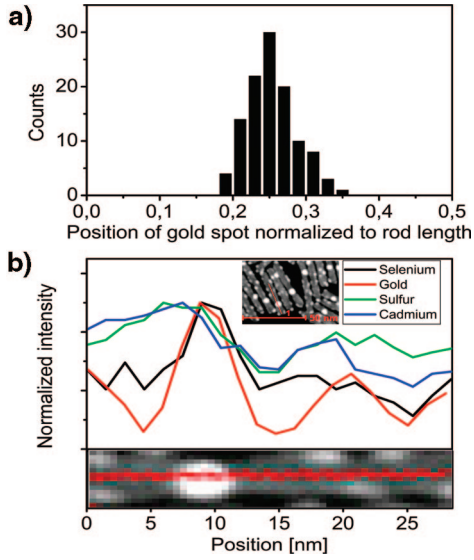

Figure 2. (a) Histogram of the seed position relative to the length of the rod; (b) elemental analysis (EDS line scan, 1.5 nm step size) of a single nanorod with a big gold dot.

This effect is visualized in Figure 2a, where a histogram of the normalized position of the larger gold dot with respect to the rod length is presented. Although a random distribution should give a constant count rate between 0 and 0.5, we observe a clear maximum at 0.25 ± 0.03.

The gold growth on seeded rods with different dimensions was also studied. Long rods (images g and h Figure 1, 108 nm long, 4.6 nm wide) and shorter thicker rods (images e and f in Figure 1, 28 nm long, 8 nm wide) were used as templates for Au growth. The long rods, with a thin CdS shell, also show very clearly located preferential Au growth. The rods with the thick CdS shell, however, show dominance

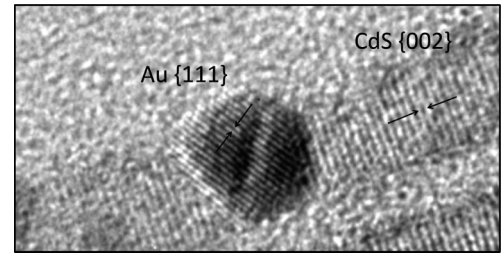

Figure 3. HR-TEM analysis of a single nanorod.The *d* spacings measured are 0.241 nm for Au (111) (literature value 0.236 nm) and 0.341 nm for CdS (002) (literature value 0.335 nm).

of growth of small Au spots, distributed on the rod surface, which resemble previous observation of growth on surface defects in CdS rods.[7]

Further characterization was provided by the HR-TEM image (Figure 3) showing that both the rod and the big gold dot are crystalline. The rod grows along the *c*-axis of CdS hcp (perpendicular to the (002) planes) and the gold growth is in the fcc structure. The *d* spacings measured from the HR-TEM in Figure 3 match very well with the corresponding bulk values for the (002) planes of hcp CdS and the (111) planes of fcc Au. Figure 2b shows an elemental analysis of a single rod with one large gold dot, along the line scan indicated in the image. The correlation of the maximum in Se content and gold content, both at the position of the large gold dot, provide strong proof for its location at the CdSe seed position. This position for the Au growth onto the CdSe seed is consistent with the earlier study of Manna et al., who found an average seed position between 1/4 to 1/3 of the rod length, in good agreement with our value of 0.25 ± 0.03 for the seed position (in medium sized rods). Moreover, the standard deviation in the normalized seed position is remarkably low demonstrating the high uniformity of the seeded

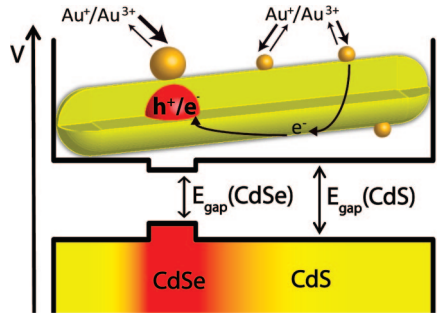

Figure 4. Scheme and potential diagram for the CdSe seeded CdS rods, along with a schematic of the electrochemical ripening mechanism for gold growth.

rods, not only in terms of dimensions but also in terms of seed location.

The optical spectroscopy performed on the structures (see Figure S1 in the Supporting Information) shows that the initially strong band gap fluorescence originating from the CdSe seeds is completely quenched upon gold growth. This is consistent with the close contact of the gold to the CdSe seed leading to fast transfer of photogenerated electrons to the Au followed by nonradiative decay.

We next consider possible mechanisms for the selectivity of gold growth at the seed position. Figure 4 shows a schematic drawing of the CdSe seeded CdS nanorods and the corresponding potential scheme for the valence and the conduction bands. In the CdSe seed region, there is a potential minimum for both the electron and the hole (type I band-alignment). Therefore, in the excited state of the nanocrystal, both charge carriers will be localized in the CdSe core (even so the electron will show a stronger delocalization due to its lower effective mass).[19] Hence a photochemical mechanism may be one of the possible options to explain the findings, where an electron in the conduction band generated through photon absorption, takes part in the reduction of the gold. Recently, Dukovic et al. reported photochemical growth of Pt on the heterostructure yielding selective growth at the seed region.[21]

In the present case, Au growth experiments carried out in darkness showed similar behavior and therefore a different growth mechanism needs to be invoked. An additional possibility is that due to the lattice mismatch between CdSe and CdS, the seed region exhibits higher crystal strain and therefore most likely contains more surface defects than the rest of the rod. These crystallographic defects can serve as sites for gold nucleation. However, this effect does not seem to be the dominant one, since ZnSe seeded CdS nanorods[22] do not show any preferential growth location, even though the seed region is shown to be more defective than in the case of CdSe seeded rods (see Figure S2 in the Supporting Information).

We next consider an electrochemical ripening mechanism as schematically shown in Figure 4. Here, gold initially grows on surface sites but at a critical size, fluctuations lead to the ripening effect where gold from a small dot dissolves in an equilibrium reaction through oxidation from the nanorod. The electrons of this oxidation reaction remain on the nanorod and will have a maximum of their probability of presence in the region of the CdSe because of the potential minimum. Hence the electrons located at the seed position can induce preferential reduction of gold, resulting in faster gold growth at this position. The Au^{3+}, which is reduced at the seed location, originates from excessive precursor in the solution and only in small parts from the small gold dots; indeed, at lower gold precursor concentration much less preferential growth can be identified. It should be noted, however, that even though the gold growth is clearly preferential to the CdSe seed position, there are still smaller gold dots located over the rod at long times (Figures S3−S7 in the Supporting Information).

To further investigate the mechanism, we followed kinetics of the growth by TEM analysis (Figure S3−S7 in the Supporting Information). At early times (1min), small Au dots are dominant. The large Au dot is seen to develop and grow in increasing percentage of the rods with time. The average number of small gold dots is somewhat smaller at all times for the rods with large gold dot compared with rods without such a large dot (e.g., after 10 min, 15 versus 12, respectively. See Table S1 and Histogram S3 in the Supporting Information). This is the expected trend from ripening but the reaction conditions are such that excess gold is present in solution which usually suppresses complete ripening. Moreover, the small Au dots at other locations may be strongly bound to the rod defect sites and not easily completely removed.

This mechanism also explains the observation that the effect of located growth becomes less dominant for rods with a thicker CdS shell (images e and f in Figure 1)). The electrochemical ripening mechanism will not be as effective with a thicker CdS shell, because the CdS shell is a potential barrier for the electron located in the CdSe seed and therefore reduces the amplitude of the electron wave function at the surface exponentially with increasing shell thickness.

Summarizing, we have demonstrated the localized growth of gold dots onto CdSe seeded CdS nanorods. The position of preferential gold growth correlates with the location of the CdSe seed. This phenomenon also allows determining that the position of the seed in the seeded rods is very well defined, at 1/4 of the rod length. An electrochemical Ostwald ripening mechanism is invoked to explain the findings.

Acknowledgment. The research was supported by the framework of the NanoSci ERA program (project SINGLE NANOHYBRID). Dirk Dorfs is grateful to the Minerva foundation for funding.

Supporting Information Available: Experimental procedures; TEM images of Au growth on ZnSe seeded CdS rods; optical data; temporal evolution of gold growth (PDF).This material is available free of charge via the Internet at http://pubs.acs.org.

CM801702X

(21) Dukovic, G.; Merkle, M. G.; Nelson, J. H.; Hughes, S. M.; Alivisatos, A. P. *Adv. Mater.* **2008**, published online.
(22) Dorfs, D.; Salant, A.; Popov, I.; Banin, U. *Small* **2008**, *4* (9), 1319–1323.